Aero-elastic modelling of the active flap concept for load control

Vasilis A. Riziotis and Spyros G. Voutsinas
National Technical University of Athens
9 Heroon Polytechneiou str., 15780, Athens, Greece
vasilis@fluid.mech.ntua.gr, spyros@fluid.mech.ntua.gr

Abstract

The active flap concept is analysed in view of controlling fatigue loads on modern wind turbines. In closed loop, it acts additionally to power control, usually done by varying both the rotor speed and the blade pitch. The work focuses on servo-aero-elastic modelling in two scale levels: that of a typical blade section (2D) and that of the entire blade (3D). The flow is simulated using vortex methods. At section level, by means of strong viscous-inviscid interaction viscous effects are accounted for, while flap and lead-lag bending are modelled with springs. At blade level, full aero-elastic modelling is carried out. The dynamic equations are completed with the control equation for the flap deflection which is coupled with the flap load. The paper describes the formulated models and discusses the effectiveness of the active flap concept in both scales. Reduction of loads is confirmed and quantitative information is provided.

Keywords: deformable trailing edge geometry, smart blade, aero-elastic modelling, fatigue load control, free-wake modelling

1 The flap concept

Flaps are known from fixed wing aerodynamics as devices providing flight controllability. By deflecting the flap, the effective angle of attack changes and so do the aerodynamic loads. The change will depend on the extent of the flap and the deflection angle. Usually flaps cover a small part of the chord length ~10-20%. So their effect on the aerodynamic performance is regarded mild while the effort needed for the actuation of the flap deflection manageable.

On fixed wings the objectives and requirements are such that only static flap deflections are needed. Usage of flaps on rotors is rare and concerns helicopter rotors [1]. The aim is no longer flight controllability but reduction of noise and/or vibrations. Therefore flap deflections need to be dynamic; usually activated at the rotation frequency or some important harmonic. In most cases, the work reported is still at investigation level. The latest report concerns successful implementation of trailing edge flaps on helicopter blades in full scale. Flight tests of a demonstration prototype have confirmed significant noise reduction which could lead to industrial implementation of the trailing edge flap concept in future [2].

On wind turbines there is no real application of the flap concept. The partial blade pitching which was investigated in the 90's, is the closest implementation to flap deflection one can find [3]. Of course at that time the main objective was power control and not reduction of loads. Design complexities as well as increased noise emissions were found to be significant drawbacks and therefore partial blade pitching was abandoned. The interest on aerodynamic control has been recently renewed primarily with the aim of reducing fatigue loads. The idea is to add an extra control on top of the variable speed and variable (collective) pitch controls which take care of power control. To this end individual and cyclic pitching of the blade have been analyzed in [4] indicating that significant load reduction is possible. For multi MW wind turbines, the size of the blades is substantial and actuation requirements are high especially for the pitch bearing and the control response. A less demanding option is offered by the active flap concept because of its size. In particular, it is possible to actuate the flap deflection with piezoelectric devices which are mounted on the blade without the need of complex mechanical designs.

2 Recent works & outline

Recent work on trailing edge flaps specifically for wind turbine blades includes both measurements and modelling. At RISOE [5] measurements on a rectangular rigid wing equipped with flap actuators have provided proof-of-concept in static and dynamic flap deflections. The model

was placed wall-to-wall, thus corresponding to a 2D aerodynamic investigation. At Delft University similar tests are in progress [6]. The wing is now flexible and flexibilities are representative of a wind turbine blade. Besides the wall-to-wall set-up, the case of a free tip configuration is also scheduled.

With respect to modelling, in [7] the thin wing linear theory is extended to include trailing edge flap deflections while in [8] the Beddoes-Leishman dynamic stall model is accordingly modified. Modelling of this type is essential because it can be directly implemented in aero-elastic codes using blade-element momentum theory. However they are in many aspects empirical. Therefore in order to have a better understanding of the underlying mechanisms, more advanced models should be formulated.

Because of the links to fatigue loads and closed loop operation of the flap, models need to be servo-aero-elastic. In the present paper advanced models are formulated in two scale levels: that of a typical blade section (2D) and that of the entire blade (3D). Effectiveness of the active flap concept is analyzed for both scales. The analyses performed are based on data from a 5MW Reference wind turbine (RWT) (a pitch-variable speed paper case machine defined within IEA activities [9]). Compared to the case of no trailing edge flap deflection, reduction of fatigue loads is confirmed at levels depending on the control characteristics.

3 Modelling

At sectional scale, the dynamic system is defined by the flap and lead-lag displacements w, u respectively and the trailing edge flap deflection φ. Flexibility is represented by springs with constants related to the blade eigenfrequencies (Figure 1).

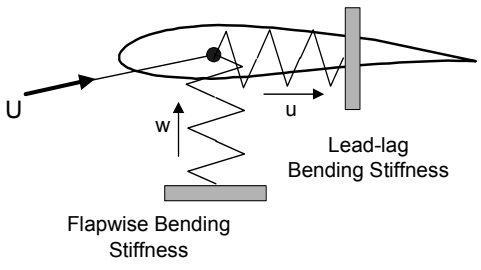

Figure 1: The typical aeroelastic section.

In non-dimensional form the elastic equations take the following form [10]:

$$\begin{bmatrix} 1 & 0 \\ 0 & 1 \end{bmatrix} \cdot \begin{Bmatrix} \ddot{u} \\ \ddot{w} \end{Bmatrix} + \kappa^2 \begin{bmatrix} \omega_u^2 - 1 & 0 \\ 0 & \omega_w^2 \end{bmatrix} \cdot \begin{Bmatrix} u \\ w \end{Bmatrix} = \frac{R_f}{2} \begin{Bmatrix} C_X \\ C_Y \end{Bmatrix} \quad (1)$$

to which the control equation for φ, is added (general expression of PID controller on the flapwise bending accelerations):

$$\begin{aligned} \dot{\varphi} &= K_P \dot{y} + K_I y + K_D \ddot{y} \\ y &= \ddot{w} \end{aligned} \quad (2)$$

In (1), displacements are referenced to the local chord c; time is referenced to c/U where U is the inflow velocity defined by the wind speed U_w and the blade speed ωr at the specific radial position; ω_u, ω_w are the lead-lag and flap eigenvalues given with reference to ω; $\kappa = \omega c / U$ and $R_f = \rho c^2 / m$ where ρ denotes the air density and m the mass of the blade per unit span length; C_X, C_Y denote the aerodynamic coefficients in the two directions of motion which both depend on $\dot{u}, \dot{w}, \varphi$ and $\dot{\varphi}$. Therefore the flow and dynamic equations must be solved iteratively.

In order to model the flow, a certain level of detail is necessary. It is important to include: the change of the geometry as well as the dynamic inflow effects induced by the pitching motion of the trailing edge flap, the plunging and lead-lag motions of the airfoil and the unsteady wake these motions will generate. An efficient way to simulate such an unsteady flow has been formulated in FOIL2W [11, 12]. Over the airfoil surface, source and vorticity distributions are defined while in the wake vortex blobs approximate the history of vorticity shedding (Figure 2).

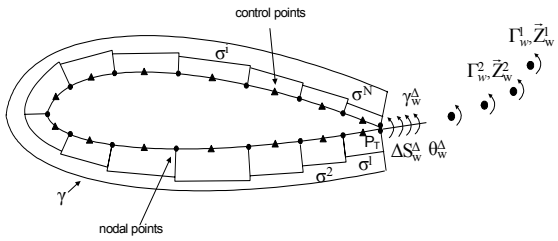

Figure 2: The inviscid flow representation.

By introducing surface velocity transpiration over the airfoil and along the wake, viscous effects can be added (Figure 3).

The transpiration intensity is determined by the solution of the deficit flow equations in integral form. Strong viscous-inviscid interaction is considered which allows valid simulations even in deep stall. Because in FOIL2W the exact

geometry of the airfoil is used, it is simple to implement the trailing edge flap deflection. It is assumed however that φ is small so that the geometry remains smooth. Therefore vortex shedding will still take place at the trailing edge. Otherwise vortex shedding due to early separation will take place upstream of the trailing edge.

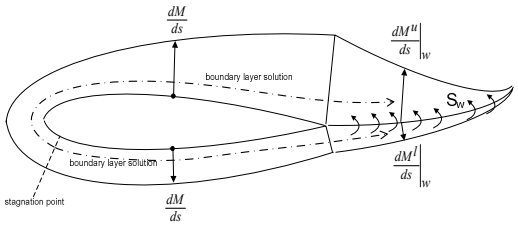

Figure 3: The transpiration velocity distribution.

At blade scale, current state of art consists of coupling BEM flow modelling with beam-type FE structural modelling in a multi-body context modularly implemented in GAST [13]. Because BEM models cannot include trailing edge deformations in a direct way, we have switched to a 3D flow model, GENUVP. It is a free-wake vortex particle flow model which has been in use for more that 10 years at NTUA [14, 15]. It consists of coupling a panel approximation of the flow induced by the blades with a vortex blob approximation of the wake. Figure 4 shows the wake generation along the trailing edge. At each time step a new wake strip is formed tangent to the emission line (left). The amount of vorticity released is determined so that at the trailing edge there is no net vorticity in accordance to the Kutta condition. At the end of the time step the wake is convected. In its new position the vortex strip (dashed wake grid) is transformed into vortex blobs while the space left is filled by the next strip (continuous line wake grid).

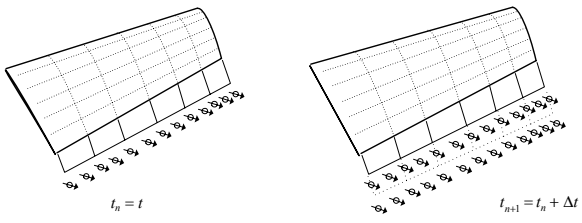

Figure 4: Wake generation and vortex blobs.

In [16], GENUVP has been coupled with the structural modules of GAST offering advanced servo-aero-elastic modelling of wind turbine configurations. This version is used in the present work. As in the 2D case, the trailing edge flap deflection is easy to implement. What is different is the shedding scheme. If vorticity is shed only along the trailing edge, when the flap is deflected, there will be rapture in the wake as shown in Figure 5a with the shed vortex sheet indicated grey. A pair of opposite vortices will appear. Their intensities will be proportional to the effective angles of attack of the sections wherefrom they are shed, while their difference corresponds to the spanwise loading distribution. If the two parts of the wake are left disconnected, the loading on both sides of the rapture will tend to zero which according to fixed wing experience this is not the case. Also during their downstream evolution they will undergo an intense roll-up subjected to strong instability. As regards the loading, a straightforward correction would be to shed $\Gamma_f - \Gamma_b$ on both sides. However this does not eliminate the intense roll-up. A more physically consistent approach is to extend vorticity shedding along the free sides (Figure 5b where the wake extension is indicated in dark grey). Note that the amount of vorticity released is such that there is no net vorticity along the shedding lines on the free sides of the blade and the flap (Kutta condition). Otherwise the structural equations are non-linearly coupled with the flow while the trailing edge flap deflection is linked to the flapwise bending, here measured at the blade tip.

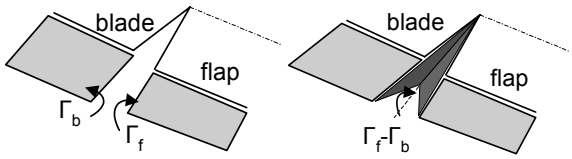

Figure 5: The shedding scheme at the flap extremities.

4 Results at sectional scale

The interest in performing 2D simulations is rather theoretical and aims at providing qualitative information which can give a better understanding of the physical mechanisms. Therefore the choice of tests has been driven by the intension to evaluate the flap concept. To this end, the NACA 64418 airfoil (employed at the outer part of the RWT blade) has been chosen at the incidence of 14 deg which is definitely high for a pitch regulated turbine. The selection of such a high incidence is justified by the fact that at lower angles (linear region of the CL curve), aerodynamic damping of the flapping motion is so high that no transient response is visible even without the controller operating. The chordwise length of the flap has been set to 10% in all test cases examined.

At first the case of an impulsive excitation is presented. It corresponds to an impulsive lock of the aero-elastic coupling. The flap and lead-lag

eigenfrequencies have been set equal to 3.5 and 5.5 /rev respectively (corresponding to the first flap and lead-lag natural frequencies of the RWT blade), R_f =0.04 and κ=0.06. Also an integral controller has been applied to the TE flap angle in closed loop with the flap bending acceleration. This choice was made in order to keep the control scheme as simple as possible since it only requires measurement of the blade acceleration which can be easily provided by an accelerometer.

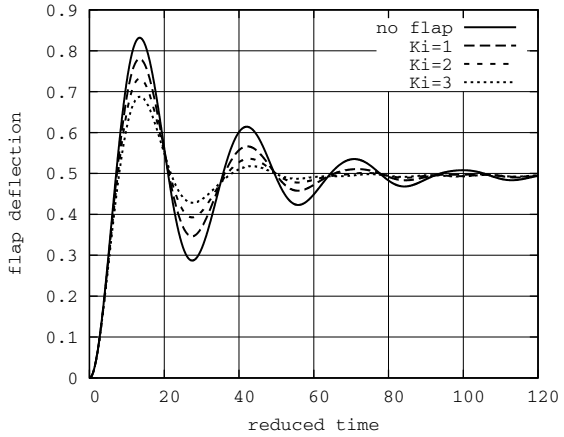

(a)

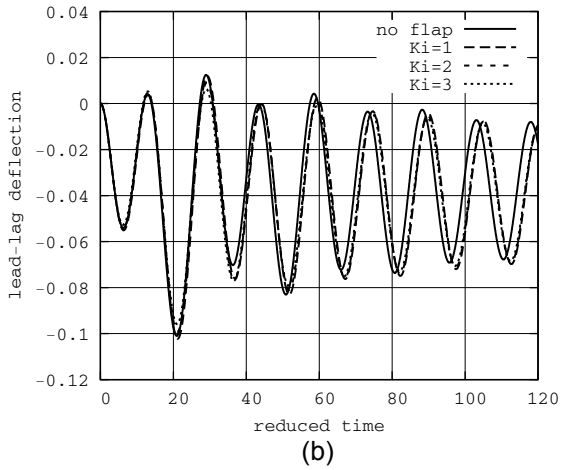

(b)

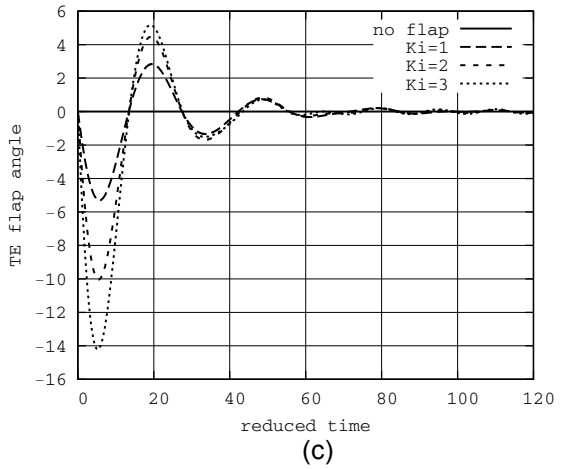

(c)

Figure 6: Structural response to an impulsive excitation.

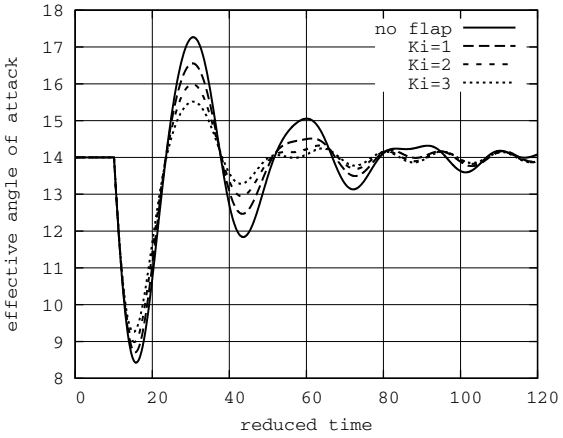

(a)

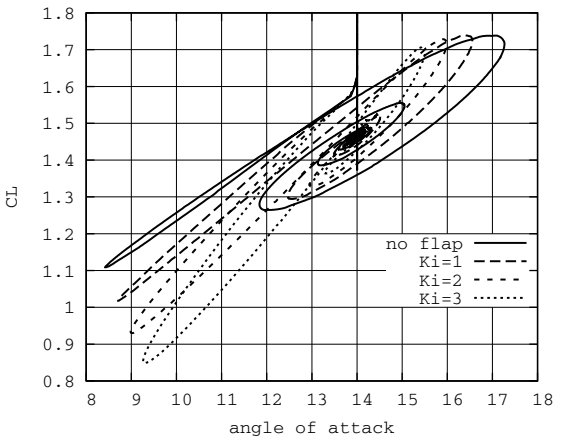

(b)

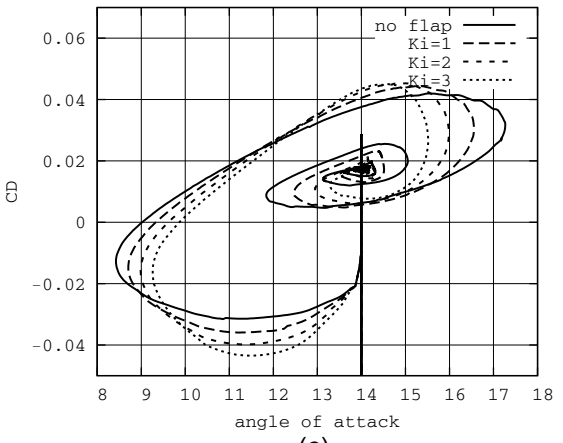

(c)

Figure 7: Aerodynamic loads response to an impulsive excitation.

In Figure 6 the structural response together with the TE flap angle is recorded for different values of the controller constant. Positive TE flap angles correspond to increasing the camber of the airfoil. There is significant reduction of the flapwise deflection at levels proportional to the value of the controller constant which is associated to increasing values of the TE flap angle. As expected the lead-lag deflection

remains practically the same. Noticeable is the high TE flap angle immediately after the locking of the aero-elastic coupling. Also important is the increase of the damping rate. In Figure 7 the load response is recorded together with the variation of the effective angle of attack.

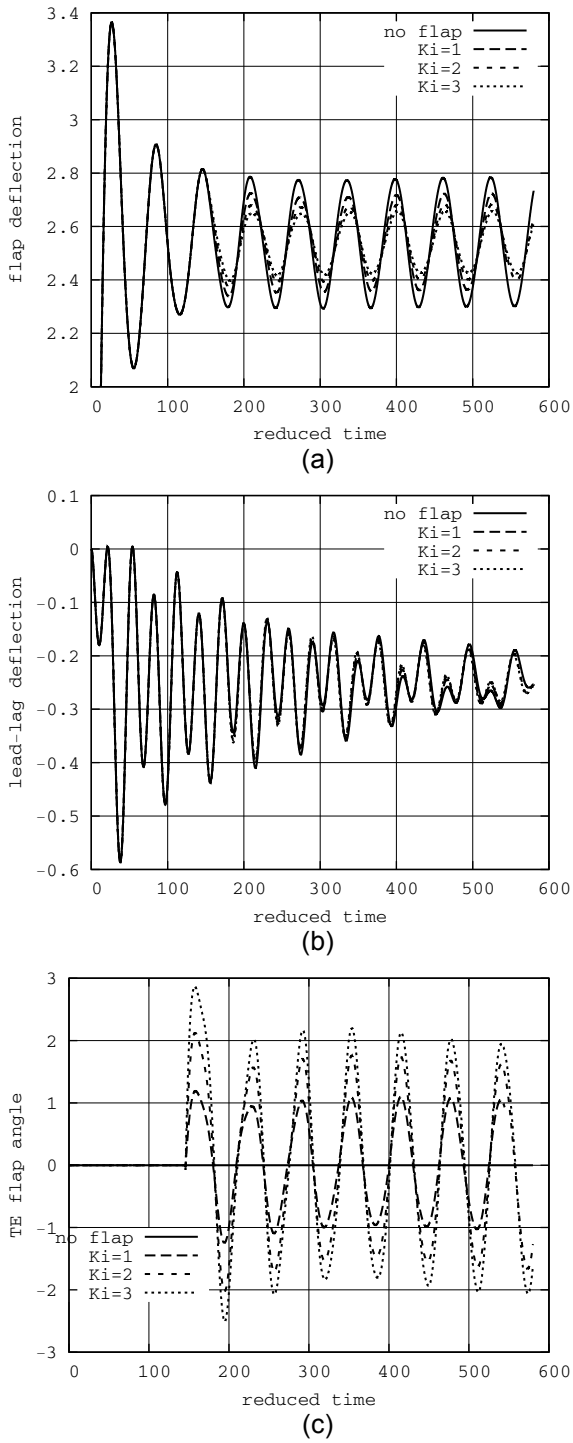

Figure 8: Structural response to a dynamic excitation.

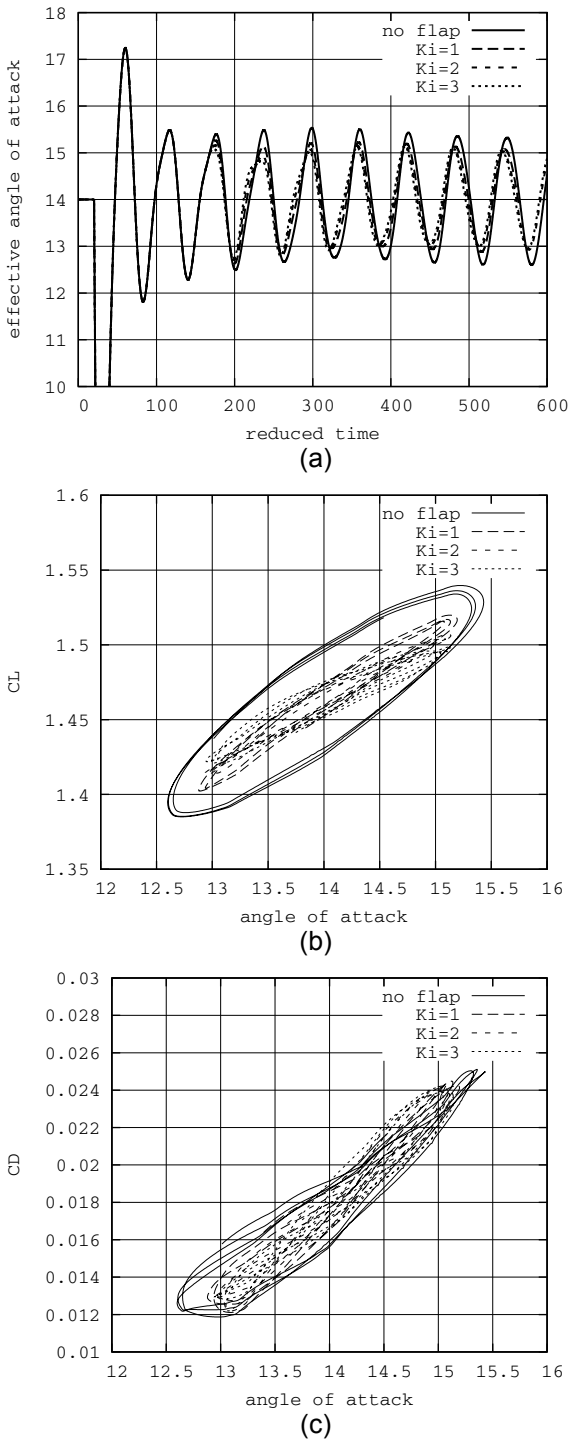

Figure 9: Aerodynamic loads response to a dynamic excitation.

The plots describe the evolution of the aerodynamics towards the final steady state. It is noted (see Figure 7b) that as the controller constant increases the slope of the initial CL loops also increases, which is indicative of the higher amount of damping introduced by the aerodynamics.

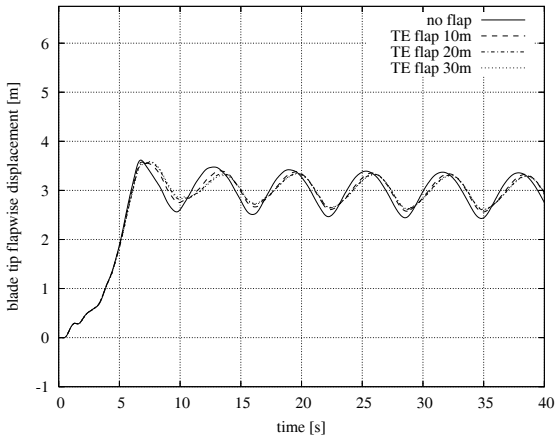

(a)

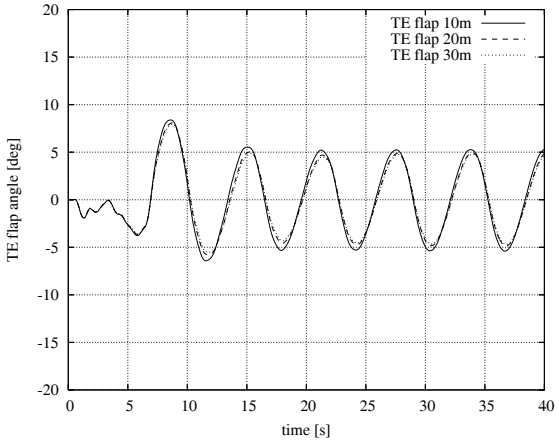

(b)

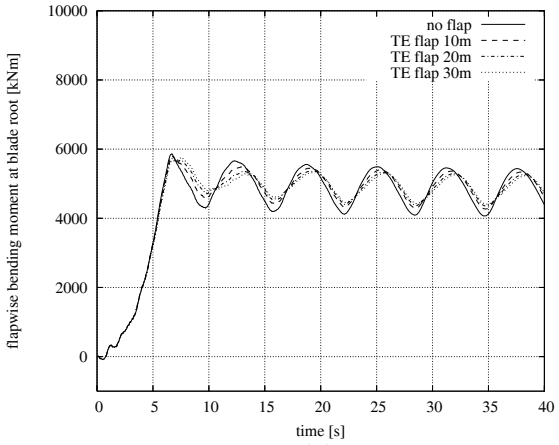

(c)

Figure 10: Wind speed=8m/s (a) tip deflection, (b) TE flap angle, (c) flapwise bending moment at blade root

The next set of results deals with the response of the system to a sinusoidal variation of the wind inflow. An amplitude of 10% at a normalised frequency of $\omega_{excit} = 2\pi f = 10$ have been selected. The frequency is not representative in the sense that wind inflow variations are expected to be at 1/rev which would lead to unnecessarily long computations given the structural eigenfrequencies. In these simulations R_f =0.07 and κ=0.04 which correspond to the RWT rotor over the span range of 80-95%. Otherwise the same recordings are shown.

As regards the structural response (Figure 8), the amplitude of the flapwise deflection is reduced at levels related to the TE flap actuation while the lead-lag deflection remains relatively unchanged. The reduction is not linear with respect to the variation of the controller constant. This suggests that in practice the design of the controller could be optimized depending on the specific turbine characteristics.

Contrary to the impulsive response, the flap angle does not exhibit an overshoot. This is due to the fact that the controller is activated at t=150 so that the system has attained an almost periodic state. Otherwise the converged amplitude of the flap angle is of the same order.

As regards the aerodynamic response, besides the initial overshoot in the effective angle of attack (Figure 9a) which is due to the sudden aero-elastic coupling activated at t=20, the system attains a periodic state fast. The effective incidence variation is in the order of ±1 deg and includes both the inflow excitation and the aeroelastic response. This explains the fact that the amplitude of the angle of attack depends on the controller constant. Then with respect to the CL loops (Figure 9b) obtained, there is a reduction in slope as the controller constant increases. This indicates that the control objective of reducing the range of variation of the lift force is accomplished. Also the slope of CD loops (Figure 9c) increases, in conformity with the higher drag forces obtained when TE flap is deflected.

5 Results at blade scale

In this section results are presented for the isolated rotor of the RWT subjected to 1/rev excitation generated by an exponential wind shear with exponent 0.2.

Simulations have been carried out for three mean wind speeds: 8m/s, 11m/s and 18m/s. The pitch and the rotor speed were set equal to their static values at these wind speeds and the power control has been switched off in order to focus solely on the effect the TE flap actuation has on the blade performance. Assessment of this effect is done with respect to the tip flapwise deflection, the TE flap angle and the flapwise bending moment at blade root (Figure 10-Figure 12). The lead-lag bending moment and the

power variation are not shown because the effect on them has been found small.

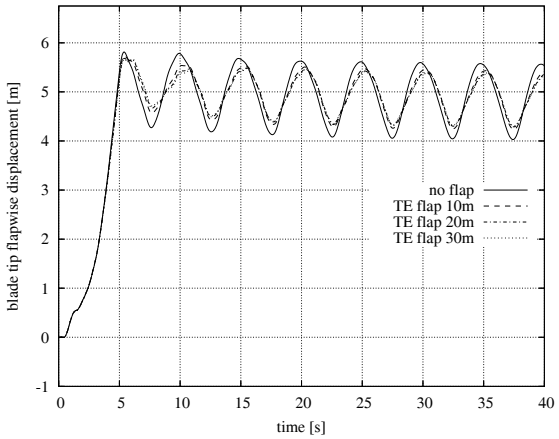

(a)

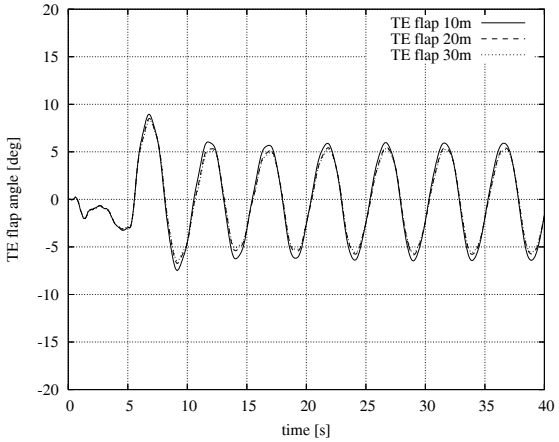

(b)

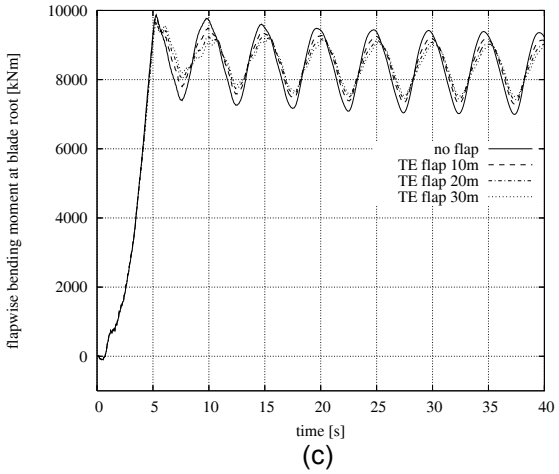

(c)

Figure 11: Wind speed=11m/s (a) tip deflection, (b) TE flap angle, (c) flapwise bending moment at blade root

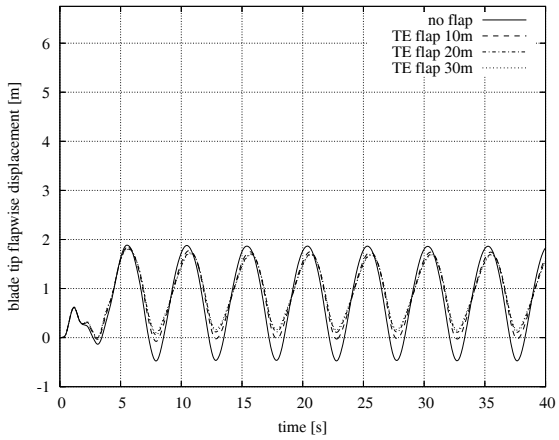

(a)

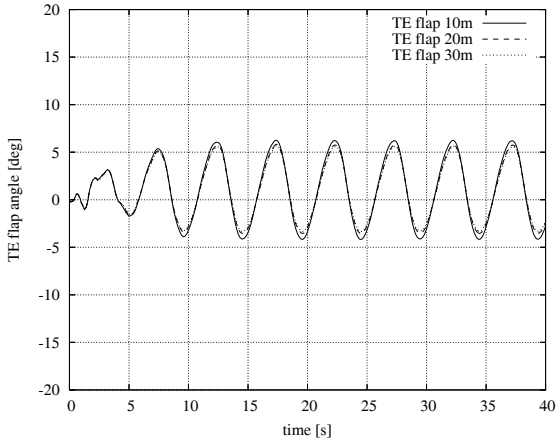

(b)

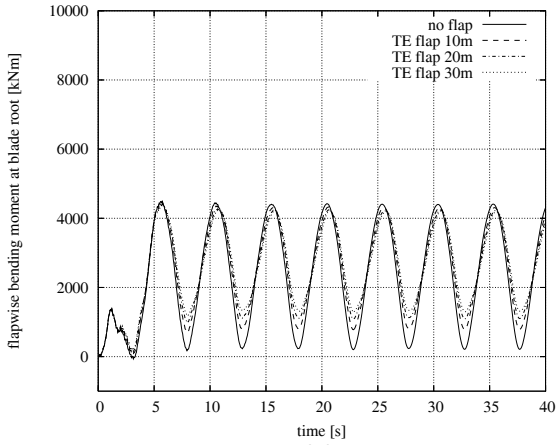

(c)

Figure 12: Wind speed=18m/s (a) tip deflection, (b) TE flap angle, (c) flapwise bending moment at blade root

Each graph contains the response without flap actuation (“no-flap”) and the responses with flap actuation in closed loop with the flap acceleration at the blade tip, for three lengths of the TE flap 10m, 20m and 30m which all end at r=60m (97.5% of the blade length). As is the 2D simulations the chordwise length of the flap is set to 10% of the local blade chord. Also in

conjunction with the 2D simulations an integral controller for the TE flap angle is assumed for all cases. The baseline value of the integral gain is set to $K_I = 2.5\times10^{-1}\ rad/(m/s)$ for wind speeds below 8 m/s. At higher speeds a gain schedule (shown in Figure 13) is applied in order to retain flap angles within a reasonable range (not exceeding the range $[-10^0, 10^0]$). This limitation imposes an upper bound to the maximum anticipated load reduction. However, it is necessary in order to avoid flow separation which is beyond the predicting capabilities of the model used. Also to avoid unnecessary actions at high frequencies, the feedback signal is passed through a bandpass filter which is centred at the rotational frequency.
At all wind speeds there is reduction in the range of the flap tip deflection and the corresponding flapwise bending load at the blade root which are almost independent of the wind speed. The maximum range reduction on loads is, as expected, obtained for the highest length of the TE flap and varies between 30%-35% depending on the wind speed. However, the benefit from extending the TE flap to bigger lengths, towards the blade mid-span, does not seem to be very significant and it definitely decreases as it moves away from the blade tip. The range of variation of the TE flap angle is similar for all wind speeds and lies in the range of $[-6^0, 6^0]$.

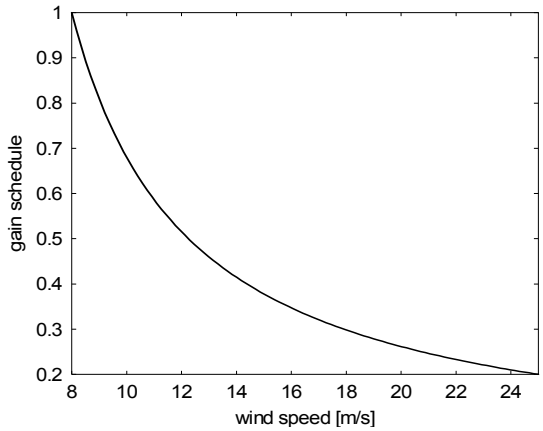

Figure 13: Gain schedule for the TE flap control.

6 Conclusions

Servo-aero-elastic models for the flap concept have been formulated in sectional (2D) and blade scale (3D). In the 2D case, response to impulsive and cyclic excitations has been considered. The implementation of a deformable trailing edge geometry in closed loop control results considerable reduction of the load to which the actuation of the trailing edge deflection is linked. The effect depends on the control limitation. Reduction of loads is directly associated to the magnitude of the flap angle. In particular the response to impulsive excitations contains an overshoot which indicates the need of careful controller design. Similar conclusions can be also drawn from the results on the rotor. It follows that deformable TE are best suited over the outboard part of the blade. Their extension in length has not an additive effect on the loads although the amplitude of the flap angle will decrease. So within the present modelling framework, the flap concept as a means of load reduction has been confirmed.

As regards the modelling itself, it allows at the lowest possible cost to obtain servo-aero-elastic simulations up to the level of the complete machine with the least of simplifying assumptions introduced. Of course direct validation is still lacking. However indirect validation of some basic aspects can be drawn from previous works. The 2D aero-elastic model was crossed checked against URANS computations in [12], while the scheme of 3D vortex shedding was again compared against URANS simulations on a tilt-rotor configuration [17].

As already indicated, the present work aimed at formulating a modelling framework and providing evidence on the effectiveness of the flap concept in reducing loads. There are several issues that need further investigation. With respect to modelling at the blade scale, viscous effects should be added. To this end, FOIL2W can be coupled on a section-by-section basis as already done in [18]. With respect to design, the behaviour of the combined pitch-variable speed-TE flap control set up must be considered especially in the case of turbulent wind inflow. Also important is to quantify the response to impulsive changes like gusts and direction changes. Finally the controller design should be considered in a realistic context.

Acknowledgements

This work was partially supported by the European Commission under contract SES6, 019945 (UPWIND).

References

[1] Friedmann, P.P. “Rotor-wing Aeroelasticity: Current Status and Future Trends”, AIAA Journal, Vol.42, No 10, October 2004

[2] Valentin Martin, W., Jänker, P., Siemetzki, M., Lorkowski, T., Grohmann, B., Maier, R., Maucher, C., Klöppel, V., Enenkl, B., Roth, D., Hansen, H. "Adaptive structures for fixed and rotary wing aircraft", Proc. SPIE Volume 6423, 2007

[3] Scheppers J.G, Snel, H. "Dynamic Inflow: Yawed conditions and partial span pitch control" Final Report of JOU2-CT92-0186 Joule II project, ECN-C-95-056 (1995)

[4] Markou, H.,Hansen, M.H., Buhl, T., Engelen, T. van, Politis, E.S., Riziotis,V.A., Poulsen, N.K., Larsen, A.J., Mogensen, T.S., Holierhoek, J.G., "Aeroelastic Stability and Control of Large Wind Turbines – Main Results," Proceedings of the 2007 European Wind Energy Conference & Exhibition, Milan

[5] Bak, C. Gaunaa, M., Andersen, P.B. Buhl, T., Hansen, P., Clememensen, K., Moeller, R. „Wind Tunnel Test on Wind Turbine Airfoil with Adaptive Trailing Edge Geometry", 45th AIAA Aerospace Sciences Meeting and Exhibit, AIAA paper 2007-1016, 2007

[6] Barlas, T.K., van Kuik, G.A.M. "State of art and perspectives of smart rotor control for wind turbines", TWIND 2007, J. Physics Conference Series 75 (2007) 012080

[7] Gaunna, M. "Unsteady 2D potential flow forces on a thin variable geometry airfoil undergoing arbitrary motion", Risoe-R-1478, Risoe, Roskilde, Denmark, 2004

[8] Andersen, P.B., Gaunaa, M., Bak, C., Hansen, M.H. "A dynamic stall model for airfoils with deformable trailing edges",TWIND 2007, J. Physics Conference Series 75 (2007) 012028

[9] Passon, P., Kühn, M., Butterfield, S.,, Jonkman, J., Camp, T. , Larsen,T.J.," OC3-Benchmark Exercise of Aeroelastic Offshore Wind Turbine Codes," TWIND 2007, J. Physics Conference Series 75 (2007) 012071

[10] Chaviaropoulos, P. K., "Flap/Lead–lag Aero-elastic Stability of Wind Turbine Blades," J. Wind Energy, 2001, 4, 183–200.

[11] Riziotis, V.A., Voutsinas, S.,G., "Dynamic stall modeling on airfoils based on strong viscous-inviscid interaction coupling," Int. J. Numer. Meth. Fluids, 56, 185-208, 2008

[12] P. K. Chaviaropoulos, P.K., Nikolaou I.G., Aggelis, K.A., Soerensen, N.N., Johansen, J.,, Hansen, M.O.L., Gaunaa, M., Hambraus, T., von Geyr, H.F., Hirsch, Ch., Shun, K., Voutsinas, S.G., Tzabiras, G., Perivolaris, Y., Dyrmose, S.Z. "Viscous and Aeroelastic Effects on Wind Turbine Blades. The VISCEL project. Part II: Aeroelastic Stability Investigations", 6, p 387-403, 2003

[13] Riziotis V.A. and Voutsinas S.G., "GAST: A general aerodynamic and structural prediction tool for wind turbines", EWEC'97 Dublin Ireland, (1997).

[14] Belessis, M.A, Chassapoyiannis, P.I., Voutsinas, S.G., "Free-wake modelling of rotor aerodynamics: Recent developments and future perspectives", Proc. of EWEC'2001, Copenhagen, Denmark

[15] Voutsinas, S.G. "Vortex Methods in Aeronautics: How to make things work", Int. Journal of Computational Fluid Dynamics, Vol 20, No 1, 2006

[16] Riziotis, V. A. and Voutsinas, S. G., "Advanced Aeroelastic Modelling of Complete Wind Turbine Configurations in view of Assessing Stability Characteristics," Proceedings of the 2006 European Wind Energy Conference & Exhibition, Athens, 27/2-2/3/2006, Edited by J. Beurskens and H. Snel, pp 46-51, 2006.

[17] Visingardi, A., Decours, J., Khier, W.,, Voutsinas, S.G. "Code-tocode comparisons for the blind-test activity of the TILTAERO project", 31st European Rotorcraft Forum, Florence, Italy, 2005

[18] Chassapoyannis, P. "Free-wake modeling and wind turbines", PhD Seminar on Wind Energy in Europe, Athens, September 2005